THE HIGH RESOLUTION STEREO CAMERA (HRSC) FOR MARS 96: RESULTS OF OUTDOOR TESTS

Hauber E., Oberst J., Flohrer J., Sebastian I., Zhang W., Robinson C., Jaumann, R., Neukum G.

DLR Berlin-Adlershof, Institute of Planetary Exploration, Rudower Chaussee 5, 12489 Berlin; Germany

Commission IV, Working Group 5

KEY WORDS: Photogrammetry, Camera, CCD, Pixel, Mapping, Matching, Extraterrestrial, HRSC, Mars.

ABSTRACT:

In spring 1995, the German High Resolution Stereo Camera (HRSC) for the Russian Mars 96 Mission was subjected to outdoor tests. The main objective was to verify operation of the camera and to validate the geometric and radiometric performance of the instrument. In addition, the functionality of much of the software developed for the systematic and scientific ground data processing was verified during the analysis of the test data. The tests demonstrate that the HRSC instrument and the processing software meet or exceed their design goals.

1. INTRODUCTION

In November 1996, the Russian „Mars 96" spacecraft will be launched carrying the two camera experiments HRSC and WAOSS for imaging from orbit (Neukum et al., 1995). During the design and development of the cameras, several tests have been carried out to verify the camera operation and performance. The main goal of the Extended Test Series 3 (ET3) was to obtain data in outdoor conditions as close to reality as possible. The simultaneous operation of the HRSC and WAOSS was tested as well as the acquisition and analysis of data simulating the operation of the cameras in Mars orbit. The radiometric and geometric characteristics of the camera were compared with the results of the calibration as performed in the laboratory. In this paper, we focus on the acquisition and analysis of the HRSC data.

The image data produced during this test also provided the unique opportunity to check the functionality of the ground data processing software as developed for pre-processing, decalibration, geometric correction, and matching of images obtained by the different CCD sensors of the camera.

2. THE HRSC CAMERA

The German High Resolution Stereo Camera (HRSC) is one of the principal orbiter payload instruments for the Russian Mars 96 Mission. The pushbroom scanner is equipped with a single 175 mm lens and 9 linear CCD arrays (5 panchromatic and 4 narrow-band color filters; see Table 1). The CCDs are mounted in parallel, perpendicular to spacecraft motion, providing nadir, forward, and backward looking viewing conditions for each of the arrays, respectively. In Mars orbit, image data will be acquired line by line as the spacecraft moves. The goal is to take large-scale high-resolution (~10-15m/pixel) multispectral stereo images at different phase angles. The hardware has been tested and calibrated and was delivered to Russia in Oct 1995 for spacecraft integration.

optics:	
focal length (mm)	175.0
f number	5.6
sensors:	
number of sensors	9
active pixels/sensor	5184
pixel size	7×7 µm
field of view (FOV):	
FOV per pixel	8.3 "
cross-track FOV	11.9°
stereo angle	18.9°
spectral ranges:	
outer stereo channels	675±90 nm
nadir channel	675±90 nm
photometry channels	675±90 nm
multispectral channels	
near infrared	970±45 nm
green	530±45 nm
blue	440±45 nm
red	750±20 nm
radiometric resolution:	
A/D converter bits	10
bits entering compression	8
min. gain	3.5
max. gain	2528
operations:	
min. exposure time	2.2 ms
max. exposure time	54.5 ms
pixel binning formats	1×1, 2×2, 4×4, 8×8
compression factors (factors actually achieved depend on scenery)	1.1 ... 100
max. data output rate	1.6 MB/s

Table 1: Camera parameters of HRSC

1. DATA ACQUISITION

The Extended Test Series 3 (ET3) for the HRSC camera experiment was carried out between March 1 and 17, 1995, at two separate camera locations near Lake Constance in southern Germany (where the industrial facilities of the HRSC main contractor Dornier GmbH are located) (Table 2).

In order to mimic flight conditions, the assembly was mounted on a slowly rotating table in a way that the line sensors were aligned perpendicular to the horizon (Fig. 1). The camera was rotated around azimuth angles from 45° to ≥ 90° with the scan rate of the camera and the rotation rate of the table selected to be similar to the viewing conditions

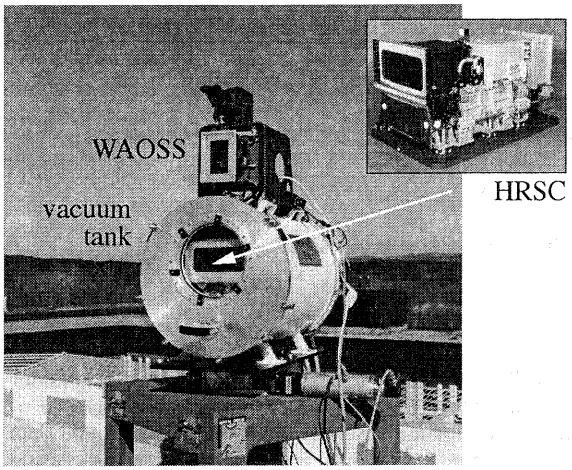

Figure 1: Test assembly at the first camera location. HRSC is enclosed in a vacuum tank in order to simulate conditions in space. WAOSS (Wide Angle Optoelectronic Stereo Scanner) and a video camera are attached on top of HRSC.

expected in Mars orbit. The experiment produced about 50 panoramic views with maximum sizes of up to 150,000 lines, each line containing up to 5,184 active pixels. High rate DCT (Discrete Cosine Transformation) data compression was applied during imaging with compression ratios of up to 40 depending on a selected quality factor, the selected code tables, and the scenery. Typically, compression ratios were selected to be small for the color channels to retain optimum radiometric accuracy. The images (Fig. 2) cover a large part of Lake Constance and the Swiss Alps.

	First location	Second location
North	47° 40.25'	47° 36.66'
East	9° 23.54'	9° 35.96'
Altitude:	425 m	434m

Table 2: Geographic coordinates of camera locations.

2. DATA PROCESSING

All images were systematically processed which included verification of telemetry data, sorting of house-keeping and sensor data, data decompression, computing of time tags for each recorded image line, and correcting for flat-field effects (Oberst et al., 1994).

In order to analyze the geometric properties of the HRSC imagery, the disparity of respective image pairs were analyzed by digital image matching. Two different area-based matching programs were available: (1) Gotcha, developed at UCL (University College London) (Day et al., 1992); and (2) CLTMATCH2, developed by TUB (Technical University of Berlin) (Oberst et al., 1996). Since CLTMATCH2 is a precursor program to the software designed to be used in the HRSC/WAOSS ground data processing, the images acquired during ET3 provide a good opportunity to test this software.

3. RADIOMETRY

3.1. General Image Quality

Sporadic consistency checks on the large amount of available data show that the general appearance of image data is excellent. The images are well focussed, and the exposure times were selected properly. However, due to the wide dynamic range in brightness of the scenery, small parts of the image are saturated or underexposed. There are no missing or extra lines. Pixel binning and changes in exposure time perform as required acording to camera commands. The excellent MTF (Modular Transfer Function) of the HRSC yields sub-pixel resolution in regions with high image contrast (Fig. 3).

3.2. Brightness Comparison

To verify the radiometric performance of the HRSC, image brightness of the five panchromatic CCD sensors have been compared. Histograms of DN for a subscene of an ET3 image (Fig. 4) demonstrate that variations in brightness between the images of the single CCD sensors are relatively minor and the overall shape of the histograms is identical. The fact that images obtained by the off-nadir channels appear darker than the nadir channel images (see detail of Fig. 4) can well be explained by the metric properties of the camera and by the imaging geometry (see 4.2). The result indicates that the radiometric performance of the HRSC is extremely accurate even for raw images.

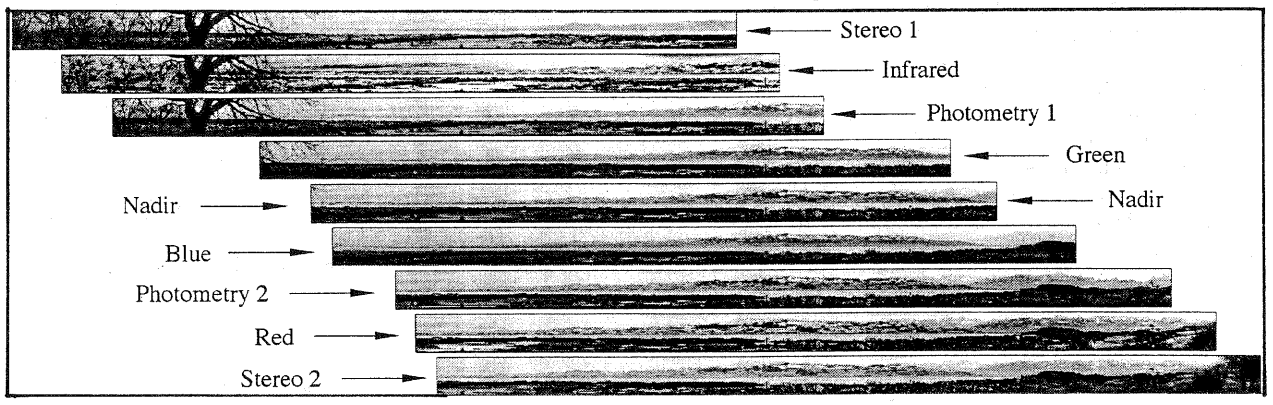

Figure 2: Example of ET3 Imaging Sequence viewing Lake Constance and the Swiss Alps. The single channels are all individually contrast enhanced, resampled to a common macropixel format, and arranged in a way that identical objects observed by different channels appear vertically aligned. Note that the direction of the rotation was from right to left.

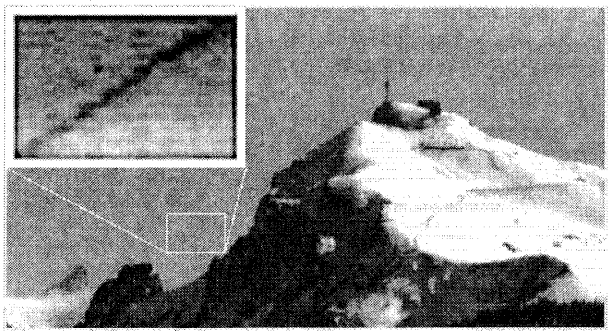

Figure 3: Detail from an ET3 image (nadir channel) showing the summit of the Kronplatz in the Swiss Alps. The blocky appearance (blow-up in the upper left corner) is due to the effects of DCT data compression. Note that although the diameters of the cables (assiciated with cable cars going to the Kronplatz) are below the nominal resolution of the camera, they are clearly visible in the image. The distance from the camera location to the summit was about 40km

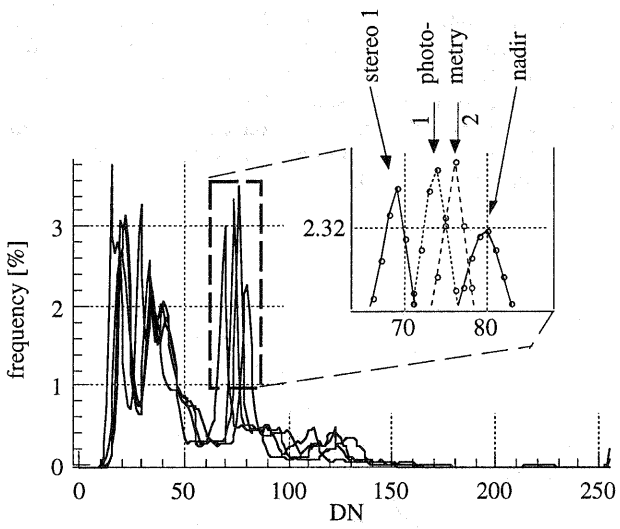

Figure 4: Histograms of panchromatic channels nadir, stereo 1, and photometry 1 and 2, respectively.

3.3. Performance of the Flat-Field Correction

During the analysis of data from HRSC Extended Test 3 all images were corrected for the different responsitivity of sensor elements (Fig. 5). These "flat-field errors" are visible in the uncorrected images as characteristic vertical stripes, which, after the flat-field correction, are effectively

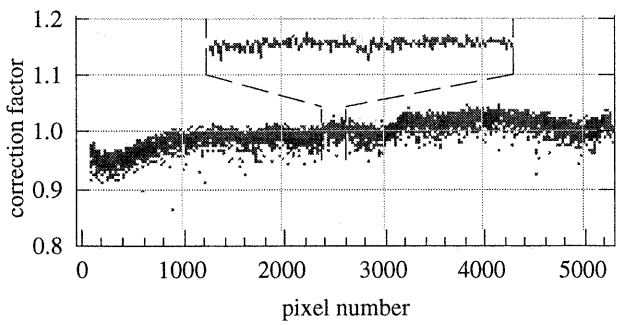

Figure 5: Flat-field correction factors for sensor 1N (nadir) as determined during the radiometric calibration.

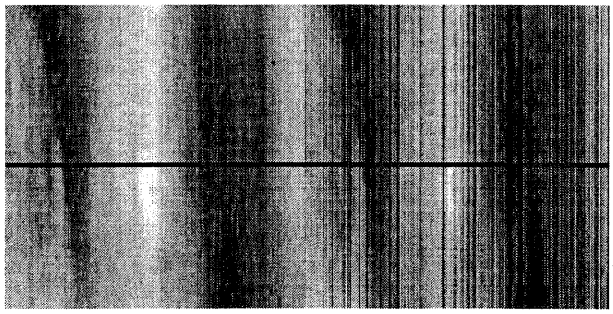

Figure 6: Detail of an ET3 imaging sequence (nadir channel) before (left) and after (right) flat field correction. Note that the contrast in the images is enhanced. The difference between adjacent pixels is typically less than 2-3 DN values, i.e. only about 1% of the total DN range. The horizontal line through the image shows the location of the profile plotted in Fig. 7.

removed. The performance of this correction has been verified plotting the DN values along a profile in the direction of the CCD sensor line before and after the flat-field correction. To minimize the effects of texture, a profile was selected which contains a relatively homogeneous sky region (Figs. 6 and 7). The profiles show that much of the high-frequency noise in the image is removed.

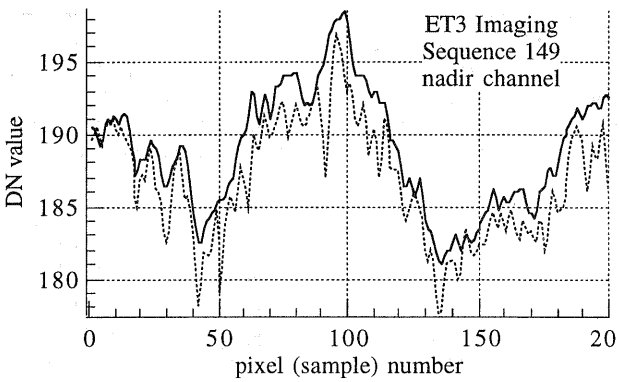

Figure 7: Brightness profile through the sky (see Fig. 6) in the nadir image: The pixel (sample) number is plotted against the respective DN values before and after the flat-field correction. It is evident that the high-frequent noise in the uncorrected image (dotted line) is effectively removed in the corrected image (solid line).

3.4. Simulation of Imaging Conditions in Mars Orbit

During selected imaging sequences, the rotational speed of the turntable was gradually increased in order to simulate the changing spacecraft speed as expected in the highly elliptical Mars orbit. The scan rate of the camera was changed accordingly in several steps, resulting in increasingly smaller exposure times for the scan lines and a decrease in image brightness.

To verify this type of camera operation, profiles of greyvalues (DN values) through homogeneous sky regions were sampled in flight direction (Fig. 8). The profiles show indeed a correspondence between exposure times and observed brightness. Additionally, this test could be used to verify the correct operation of the software which computes

time tags and exposure time data for each image lines. No divergence between changes of exposure times, as indicated in the housekeeping data, and drops of DN values could be found.

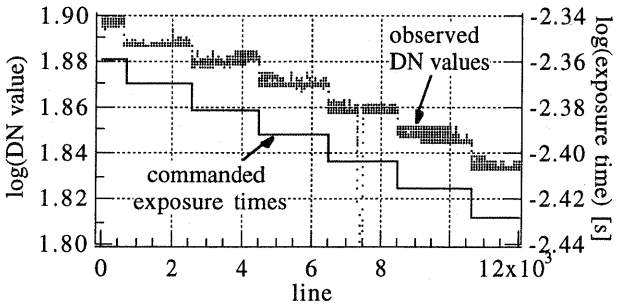

Figure 8: In order to verify proper changes in exposure time during imaging, pixel greyvalues are plotted along a sky profile in line direction. Indeed, each change in the integration time (solid line) is clearly visible as a decrease in brightness by the corresponding magnitude in this logarithmic plot. The prominent feature at line ≈7,400 is an artifact.

4. GEOMETRY

4.1. Camera Coordinate System

For a geometric analysis of all HRSC channels, we first thoroughly analyzed the setup of the experiment. Initially, we assumed that the origin of the camera coordinate system (Fig. 9) was located in the center of the rotational axis and that the camera was somewhat offset from the origin of this system, and in addition, tilted towards the observed scenery.

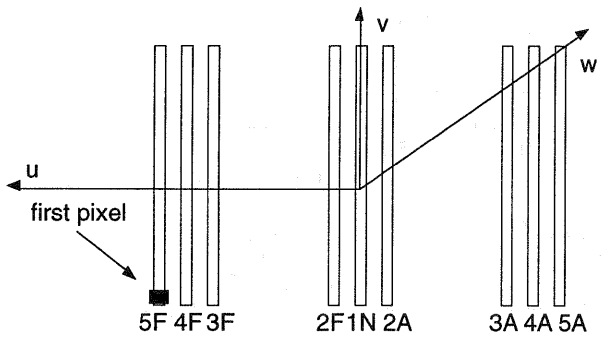

Figure 9: Camera coordinate system of HRSC as used in this paper. Flight direction is u, the optical axis is w, and v is parallel to the orientation of the CCD lines (5F stero 2, 4F red, 3F photometry 2, 2F blue, 1N nadir, 2A green, 3A photometry 1, 4A infrared, 5A stereo 1).

We collected large numbers of tiepoints in the nadir and the two stereo channels and performed a least squares adjustment to determine the offset and the angle. While the offset was found to be small and insignificant for the analysis to follow (0.028 ± 0.0023mm), the angle was found to be within -0.09039° ± 0.0007°.

4.2. Camera Metric Properties

HRSC is a metric camera (Fig. 10). This implies that during operation from orbit, all pixels –even though on different CCD lines– will have the same areal coverage on the planet's surface, assuming that the surface is planar. As a consequence of camera metric properties, each pixel's field-of-view will differ according to the pixel's position on the focal plane. It was one of the goals of ET3 to verify this property of the camera, which is an important hardware requirement for photogrammetric processing of imagery.

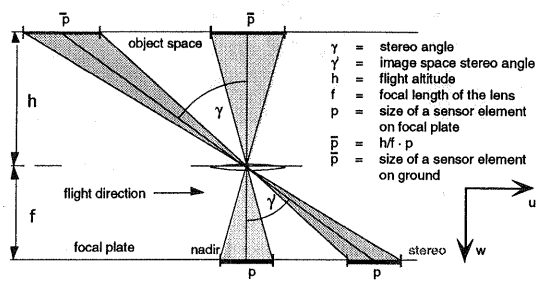

Figure 10: Metric properties of HRSC: Relationship between sensor element field of view and ground pixel size

In order to verify this characteristics, we took advantage of the camera rotation during the ET3 experiment. Unlike during a flight above a planar surface, ground pixel sizes for sensor elements of the stereo and nadir channel, respectively, will differ substantially (Fig. 11) in this geometry. In the following, we concentrate on the stereo and nadir channels. Howewer, the same considerations apply to the other channels as well.

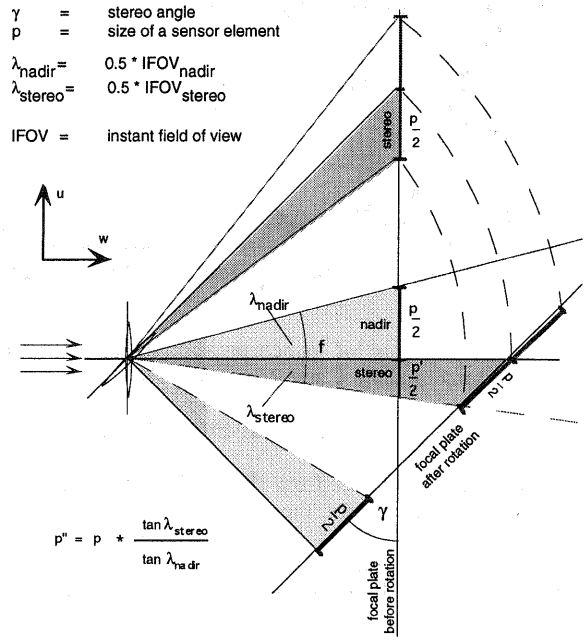

Figure 11: Relationship between ground pixel sizes in CCD channels for a rotating HRSC.

From Figure 11, we determined that the field of view of stereo pixels is about 10% less than that of the nadir pixels. This results in darker images from the stereo channels relative to the nadir channel. This offset in the brightness level of the off-nadir channels, including the photometry channels, is clearly observed in the histograms of the images (cf. Fig. 3).

Likewise, due to smaller fields of view of pixels located on the stereo CCD line (Fig. 11), an object will cover a larger

number of sensor elements on the stereo than on the nadir CCD line (Fig. 12).

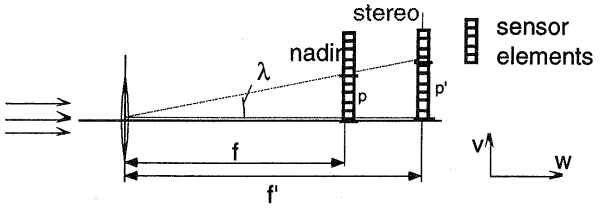

Figure 12: Effect of camera rotation on the resolution of a sensor element in v direction (perpendicular to the direction of spacecraft motion)

- λ angle covered by an object
- f focal length of the lens
- f' changed focal distance due to camera rotation (f'=f/cos γ)
- p distance covered on nadir channel (p = tan λ*f)
- p´ distance as projected onto the rotated focal plate (p´= tan λ*f´)

Hence, an object viewed by the stereo channels is "elongated" in *v* direction with respect to the nadir channel (Fig.13), i.e., a circle in the nadir channel appears as an ellipse in the stereo channel, with the long axis oriented parallel to the direction of the CCD sensors (*v* direction).

We used digital image matching to identify and to quantify this type of distortion in the imagery. The stereo channel 1 of an ET3 image was matched to the nadir channel (Fig. 14). With the stereo angle being 18.94°, we estimate that elongation of features in stereo channel images with respect to nadir images should be about 5% (cf. Fig. 12). This agrees with what is seen in the disparity data (Fig. 14).

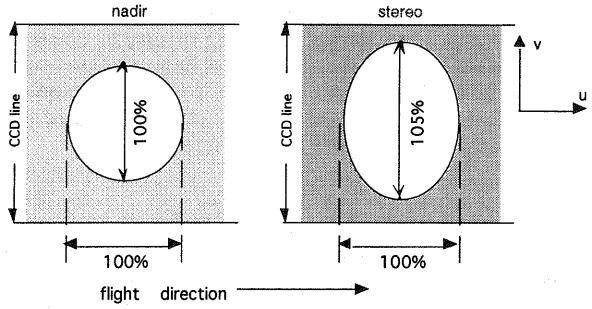

Figure 13: Effect of camera metric properties on scanner images obtained by camera rotation: features in off-nadir images are elongated perpendicular to the direction of the rotation. Due to the smaller pixel field of view the stereo channel image is darker.

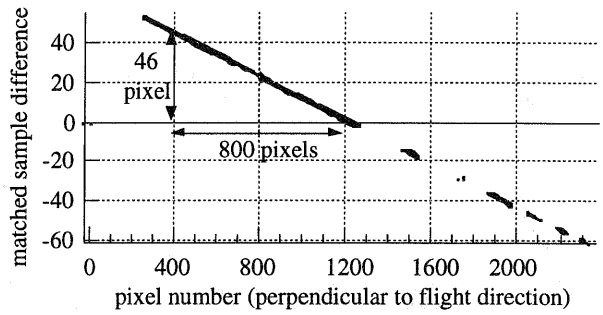

Figure 14: Plot of reference sample numbers versus the difference of matched sample number to matched sample number (reference image: nadir channel; matched image: stereo 1 channel). These disparity data demonstrate the metric properties of the camera, in particular the decreasing field-of-view for off-nadir pixels (cf. Figs. 11 and 12).

4.3. Verification of Geometric Calibration

The camera tests provide the unique opportunity to verify the geometric precision of the instrument. The calibration data indicate that the nadir, the stereo 1, and the stero 2

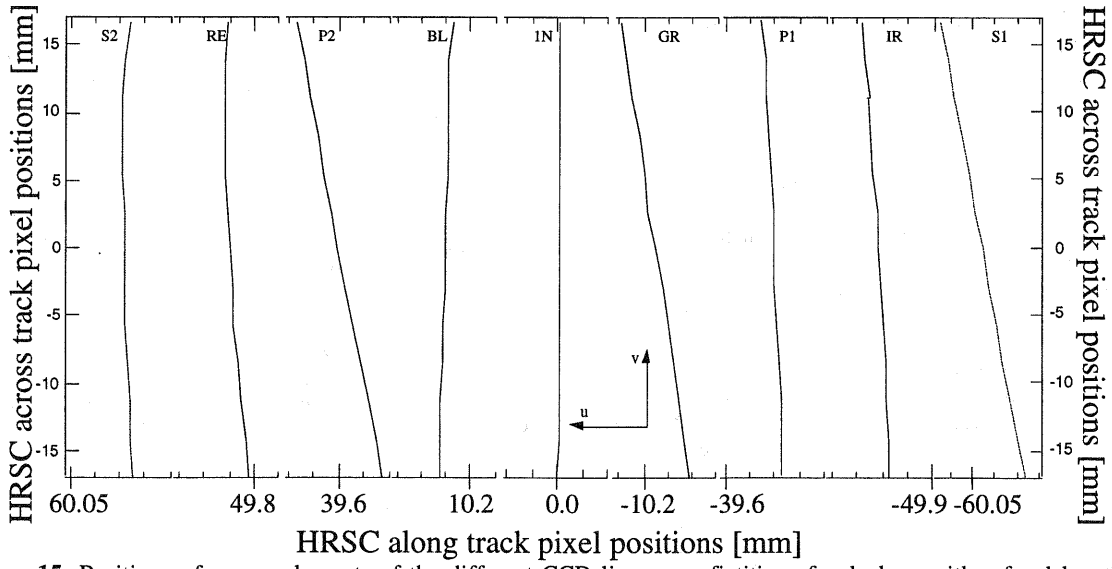

Figure 15: Positions of sensor elements of the different CCD lines on a fictitious focal plane with a focal length of 175 mm.

channels are not arranged perfectly parallel on the focal plane plane (Fig. 15). Hence, matching of images obtained by different CCD lines (oriented in an oblique direction with respect to each other on the fictitious focal plane) should produce disparity data with a similarly oblique trend of the matched pixels relative to the original referenc
pixels.

In Figure 16, the results for automatic matching of parts of the stereo 1 and 2 channels to the nadir are shown for a selected image line. The nadir channel is the reference channel and is not plotted in the diagram (it can be thought as a horizontal line at a difference of 0). It is evident from the plot that the pixel positions on the stereo 1 and stereo 2 CCD lines have distinct trends towards increasing and decreasing offsets to the pixel positions in the nadir channe, respectively, as is expected from the orientations of CCD lines in the focal plane (Fig. 15). Hence, these data provide a crude qualitative check on the geometric calibration.

The test also shows that the matcher achieves ist design goal to obtain disparity data with subpixel accuracy.

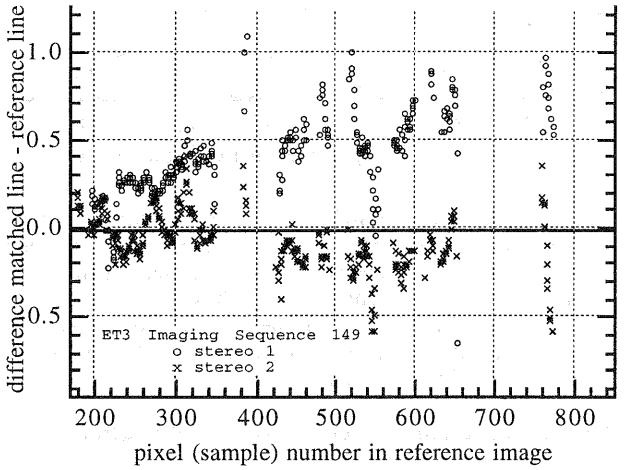

Figure 16: Pixel number of reference image (nadir channel) vs. difference between line number in the matched images (stereo channels 1 and 2, respectively) and the reference image. The scattering of the plotted values around the observed trend is attributed to atmospheric turbulences caused by large temperature gradients over the surface of Lake Constance (see Discussion).

5. SUMMARY AND DISCUSSION

The HRSC camera which is going to be launched to Mars in November 1996 was operated successfully in the first outdoor test. The results demonstrate that HRSC, for the test cases that were studied, fully meets the design goals.

The instrument operates properly (pixel binning, change of scan rate) according to camera commands. Image data in the panchromatic channels are highly reproduceble. The expected effects of the camera rotation on the brightness levels are being confirmed by the test data. The flat field files determined during radiometric calibration appear to correctly describe the different responsitivity of sensor elements. The correction significantly improves the image quality. Compression/decompression artifacts are visible, but negligible. They do not appear to affect the further processing, e.g. the flat-field correction and image matching. We also carried out a successful rough verification of image scale and resolution and verified the general properties of camera metric properties and the geometric calibration data.

Finally, ET3 also provided an important verification of the flight software. We verified the correct operation of parts of the preprocessing software, the decompression code, the flat-field correction and the software that computes time tags for each image line. All software modules were found to fulfill the requirements. The digital image matcher, an important cornerstone program of the photogrammetric processing, works according to the design goals. Large contiguous image areas can be "mapped" and pixel coordinates of conjugate points can be determined at sub-pixel level. It is noted that scattering of the disparity data are seen in the images. However, we carried out independent tests using the Gotcha matcher (Day et al., 1992) which gave similar results, indicating that the scattering does not represent artifacts generated by the matching software. Instead, we think the scattering at sub-pixel level to be due to atmospheric turbulences caused by large temperature gradients over the surface of Lake Constance.

More thorough analyses of the test data are currently under way, as at the current state of this study and within the limited time available, no comprehensive, but only sporadic checks could be done on the huge amount of image data that was collected. However, for complete analysis of the performance of HRSC and the ground data processing system, more sophisticated tests must be conducted. For this purpose, an airborne experiment using the HRSC flight spare model will be carried out near Mount Etna in Sicily, Italy, later this year. The goal of the experiment is to acquire a data set which can be subjected to a full photogrammetric analysis, resulting in large-scale digital terrain models (DTMs) and color ortho image mosaics.

Acknowledgements: We wish to thank our co-workers T. Roatsch, G. Schwarz, C. Reck, and the Dornier Test Team who provided much help in the acquisition and processing of the ET3 data. We also wish to thank our collegues at the Technical University of Berlin for important software contributions for this study.

6. REFERENCES

Day, T. et al., 1992. Automated Digital Topographic Mapping Techniques for Mars. In L.W. Fritz and J.R. Lucas (Ed.), *International Archives of Photogrammetry and Remote Sensing,* 29(B4), pp 801-808, Washington D.C.: American Society of Photogrammetry and Remote Sensing.

Neukum, G. et al., 1995. The Multiple Line Scanner Camera Experiment for the Russian Mars 96 Mission: Status Report and Prospects for the Future. *Photogrammetric Week '95,* pp. 45-61, Heidelberg: Wichmann, 1995.

Oberst, J. et al., 1994. Mars '94/96 Pushbroom Cameras: Plans for Ground Data Processing and Analysis. Proceedings of the Symposium "Mapping and Geographic Information Systems", ISPRS, Vol. 30(4), pp. 533-540.

Oberst, J. et al., 1996, Photogrammetric Analysis of Clementine multi-look-angle images obtained near Mare Orientale, Planet. Space Science, in press.